Available online at www.sciencedirect.com
ScienceDirect
Journal of Hazardous Materials 150 (2008) 124–135
Journal of Hazardous Materials
www.elsevier.com/locate/jhazmat

Behavior of aluminum electrodes in electrocoagulation process

G. Mouedhen [a], M. Feki [a], M. De Petris Wery [b], H.F. Ayedi [a,*]

[a] *Unité de Chimie Industrielle et Matériaux (UCIM), ENIS, B.P.W. Sfax, Tunisie*
[b] *IUT Mesures Physiques d'Orsay, Plateau du Moulon, 91400 Orsay, France*

Received 21 December 2006; received in revised form 16 April 2007; accepted 17 April 2007
Available online 24 April 2007

Abstract

In the present work, electrocoagulation process with aluminum electrodes was investigated. Different operational conditions such as composition of Na_2SO_4 based solutions, pH and current density were examined in a systematic manner. Their influence on (i) electrode polarization phenomena, (ii) pH evolution during electrolysis and (iii) the amount of Al released (coagulant) was investigated. For this purpose, potentiodynamic tests and electrolyses using different electrochemical cell configurations were conducted. It is mainly found that (i) a minimum Cl^- concentration of the electrolyte of about 60 ppm is required to breakdown the anodic passive film and considerably reduce the cell voltage during electrolysis; (ii) the anodic dissolution efficiency is unit; (iii) the global amount of coagulant (Al^{3+}) generated has two origins: electrochemical oxidation of the anode and "chemical" attack of the cathode and (iv) electrolysis with Al electrodes acts as pH neutralization of the electrolytic medium.Taking into account advantage of the pH evolution observed during electrolysis, electrocoagulation tests were performed to treat a synthetic wastewater containing heavy metallic ions (Ni^{2+}, Cu^{2+}, Zn^{2+}). Removal efficiencies over 98% were reached. Furthermore, our results displayed prominently that an increase of current density notably reduces the treatment duration without inducing a strong increase of the charge loading.

Keywords: Aluminum electrodes; Electrochemical behavior; Electrocoagulation; Wastewater treatment

1. Introduction

Legislative and normative regulations concerning the discharge of wastewater are drastically increasing. The commonly used physico-chemical treatment processes require chemical additions and a great quantity of sludge is generated. Therefore, there is an urgent need to develop innovative and more effective techniques for treatment of wastewaters. Electrochemical techniques have attracted, in this case, a great deal of attention because of their versatility, safety, selectivity, amenability to automation and environmental compatibility [1]. Electrocoagulation (EC) appears to be one of the most effective approaches. It involves the generation of coagulant in situ by electro-oxidation of a sacrificial anode, generally made of aluminum or iron. EC, which is known as a reliable and mainly cost-effective wastewater treatment process [2,3], is characterized by simple and easy operated equipment, short operation time, none or negligible amount of chemicals and low sludge production [4,5]. The flocs formed by EC are relatively large and contain less bound water. They are also more stable. EC has been applied successfully to treat potable water [6] and various wastewaters such as oil–water emulsions [7], dye-containing solutions [8–11], urban and restaurant wastewaters [12–14]. Further, EC process has been proposed in the last decades as an effective method to remove soluble ionic species from solutions, particularly heavy metals [15–18]. However, EC technique has been investigated in these works predominantly to point out the treatment efficiency, and not so much with respect to the fundamental aspects. EC is still empirically optimized process that requires more fundamental studies to be fully exploited [19,20]. The existence of passive oxide film on aluminum anode, for example, is one of the main problems of the EC process using this metal as electrode material [6,21]. This film increases the applied potential and leads to a waste of energy in the EC process. Frequently, the treated industrial wastewaters contain most often chloride, which may lead to the dissolution of the passive film on the anode surface [22]. However, the required amount of halide ions for the dissolution of the oxide film is, in our knowledge, not yet established. Process key

* Corresponding author. Tel.: +216 274 088; fax: +216 275 595.
E-mail address: feridayedi@yahoo.fr (H.F. Ayedi).

0304-3894/$ – see front matter © 2007 Elsevier B.V. All rights reserved.
doi:10.1016/j.jhazmat.2007.04.090

Nomenclature

C_0	initial concentration of the metallic ion
C_f	final concentration of the metallic ion at moment t
d_{ie}	electrode gap
E_{corr}	corrosion potential of the electrode
E_{pit}	pitting potential of the electrode
J	current density
m_{exp}	experimental amount of aluminum released during electrolysis
m_{th}	theoretical amount of aluminum released during electrolysis
pH_f	final pH of electrolyte
pH_i	initial pH of electrolyte
RE	removal efficiency
S_{TE}	effective area of electrode
t_e	electrolysis time
U	electrolysis voltage

Greek letter

χ	conductivity of electrolyte

characteristics such coagulant level (Al^{3+}) in relation to the operating parameters (i.e. current density, pH, etc.) is also too often occulted. Furthermore, firm evidences for (i) the different origins of the coagulant (Al^{3+}) released during EC and (ii) electrochemical and chemical reactions at the electrode surfaces, have not been provided. This paucity of scientific understanding of electrochemical and chemical phenomena during EC treatment does not allow modeling of the process or the design of improved systems and limits the performance of this technique [21]. In this respect, the electrochemical behavior of electrode material in EC treatment need to be further studied.

The present work was aimed at examining further some fundamental and applied aspects of EC process using aluminum electrodes. In this regard, we first concentrated on the electrochemical behavior of the electrode material during electrolysis in Cl^--free and containing solutions with special emphasis on the minimum Cl^- concentration allowing the breakdown of the passive oxide layer. For the better understanding of some observed phenomena, electrolysis experiments were supplemented by potentiodynamic polarization tests. Then, we through more light on sources and amounts of coagulant (Al^{3+}) released during EC under different operational parameters (Cl^- concentration, pH, current density). For this purpose, electrolyses in uncompartmentalized and compartmentalized reactors with various combinations of electrode materials (Al/Al, Al/platinized Ti) were considered. Since EC operating conditions are highly dependant on the pH of the aqueous media, pH effects were also investigated. To take advantage of the pH evolution observed during electrolyses with aluminum electrodes, potentiality of EC process for removing soluble heavy metallic species was tested considering a synthetic wastewater containing Ni^{2+}, Cu^{2+} and Zn^{2+} ions.

2. Material and methods

Electrochemical behavior of aluminum was investigated via electrolyses and potentiodynamic polarisation tests using sodium sulfate as background electrolyte. Electrolyses were performed in a thermostated electrolytic cell with (i) two opposing aluminum plates served as parallel–vertical electrodes and (ii) an aluminum anode and a platinized titanium mesh cathode. Electrolyses in a compartmentalized reactor with two aluminum plates were also carried out. The anolyte and catholyte were separated by cation exchange membrane (IONAC MC 3470) in Na^+ form.

Aluminum plates were cut from a commercial grade aluminum sheet (99% purity) of 3 mm thickness. The electrode surface was first mechanically polished underwater with 400 grade abrasive paper in order to ensure surface reproducibility, rinsed with distilled water and dried prior to immersion in the electrolyte. The effective area of each electrode used for electrolysis was 30 cm^2. The electrodes were connected to a digital dc power supply with potentiostatic or galvanostatic operational options (CONVERGIE – CLES 60-3) providing current and voltage in the range of 0–3 A and 0–60 V. The current was kept constant for each run. The anode/cathode gap was kept constant at 4 cm except indication. The cell voltage was recorded using a data logger (LINSEIS L 6512). A gentle magnetic stirring rate of about 200 rpm was applied to the electrolyte in all tests. Electrolyte volume used was 500 mL. The total time duration of electrolysis was 30 min for most test runs unless noted otherwise.

Morphological observations of aluminum electrode surfaces after electrolysis tests were achieved by metallographic triocular inversed microscope (AuxiLab, model ZUZI 178) and scanning electronic microscope (Jeol JSM-6400F).

Potentiodynamic polarization tests of aluminum were performed with a three-electrode cell (Radiometer C145/170) and a potentiostat/galvanostat (PGP 20V 1A) controlled by a Voltamaster 4 software allowing data acquisition. Platinum wire was used as a counter electrode and saturated calomel electrode (SCE) with a luggin capillary as a reference one. Working electrode was a 1 cm^2 aluminum flat disc inserted into a PTFE sample holder (Radiometer PEK 29). Before each experiment, working electrode was mechanically ground using successively finer grade of abrasive paper, polished with 0.3 μm alumina, degreased in acetone, rinsed with distilled water and then dried before being inserted into the sample holder. One hour was allowed to elapse before measurements began so that the open circuit potential could reach its steady value.

Electrocoagulation experiments were carried out using two parallel aluminum electrodes (S_{TE} = 54 cm^2) and 900 mL of electrolyte. The solution pH was 4.9 and its composition was: 1000 ppm Na_2SO_4, 100 ppm NaCl, 67 ppm Ni^{2+}, 59 ppm Cu^{2+} and 67 ppm Zn^{2+}. Heavy metallic ions were introduced into solution by dissolving the appropriate amount of the corresponding sulfate salts.

All experiments were performed at 30 ± 1 °C and were triplicated.

All solutions used for the experiments were prepared from analytical grade chemical reagents (Fluka products) without any further purification. Deionised water was used in all the experimental runs.

The initial pH of the solutions was adjusted by adding either sulfuric acid or sodium hydroxide.

Solution pH and conductivity were measured using high precision pH meter, equipped with a combined glass electrode (METROHM) and electronic conductivity meter (TACUSSEL, type CD 6NG) equipped with an immersion measurement probe, respectively.

The metallic ion concentrations were determined by atomic absorption spectrometry (Zeeman spectrophotometer HITACHI Z-6100) after nitric acidification and suitable dilution of samples taken in the electrolytic solutions.

3. A brief description of EC using aluminum electrodes

It is well known that in EC process the main reactions occurring at the aluminum electrodes during electrolysis are:

$$Al \rightarrow Al^{3+} + 3e^- \quad \text{(anode)} \tag{1}$$

$$2H_2O + 2e^- \rightarrow H_2 + 2OH^- \quad \text{(cathode)} \tag{2}$$

According to many authors [13,14,18,21,23], when the anode potential is sufficiently high, secondary reactions may occur, especially oxygen evolution (Eq. (3)):

$$2H_2O \rightarrow O_2 + 4H^+ + 4e^- \tag{3}$$

Aluminum ions (Al^{3+}) produced by electrolytic dissolution of the anode (Eq. (1)) immediately undergo spontaneous hydrolysis reactions which generate various monomeric species according to the following sequence (omitting co-ordinated water molecules for convenience):

$$Al^{3+} + H_2O \rightarrow Al(OH)^{2+} + H^+ \tag{4}$$

$$Al(OH)^{2+} + H_2O \rightarrow Al(OH)_2{}^+ + H^+ \tag{5}$$

$$Al(OH)_2{}^+ + H_2O \rightarrow Al(OH)_3 + H^+ \tag{6}$$

Actually, this is only an oversimplified scheme, since dimeric, trimeric and polynuclear hydrolysis products of Al can also form: $Al_2(OH)_2{}^{4+}$, $Al_3(OH)_4{}^{5+}$, $Al_6(OH)_{15}{}^{3+}$, $Al_7(OH)_{17}{}^{4+}$, $Al_8(OH)_{20}{}^{4+}$, $Al_{13}O_4(OH)_{24}{}^{7+}$, $Al_{13}(OH)_{34}{}^{5+}$ [23–26].

Hydrolysis reactions (Eqs. (4)–(6)) make the anode vicinity acidic. Conversely, hydrogen evolution at the cathode (Eq. (2)) makes the electrode vicinity alkali.

Cationic hydrolysis products of aluminum may react with OH^- ions to transform finally in the bulk solution into amorphous $Al(OH)_{3(s)}$ according to complex precipitation kinetics [23–25]. The mode of action of the generated Al species in EC process is generally explained in terms of two distinct mechanisms: charge neutralization of negatively charged colloids by cationic hydrolysis products and incorporation of impurities in the amorphous hydroxide precipitate ("sweep flocculation"). The relative importance of these mechanisms strongly depends on pH and coagulant dosage [27].

Finally, solution chemistry has considerable influence on coagulation process. In this context, it is noteworthy that sulfate anions, in contrast to monovalent ions such as chloride and nitrate, promote markedly the precipitation of aluminum hydroxide by reducing significantly the positive charge of aluminum hydrolysis products [27,28]. It has been shown that sulfate is adsorbed but not incorporated into the aluminum hydroxide precipitate [28]. Thus, sulfate acts as a "catalyst" for aluminum hydroxide precipitation and coagulation.

4. Results and discussion

4.1. Effect of sodium chloride on aluminum electrochemical behavior during electrolysis

In order to examine the effect of chloride ion concentration on electrolysis voltage, sodium sulfate electrolytes containing different doses of sodium chloride (NaCl) were retained.

Fig. 1 shows that during the initial periods of electrolysis, the voltage increases sharply until a maximum value. After that, the voltage decreases to reach a pseudo-stationary value. Moreover, the maximum value of voltage and the duration time required to achieve the pseudo-stationary plateau are much higher with lower NaCl concentrations. The effect of NaCl concentrations on pseudo-stationary electrolysis voltage can be seen in Fig. 2. As NaCl dose increases from 0 to 100 ppm, the cell voltage decreases rapidly from 42 to 7 V. However, an additional increase of salt dose does not improve the electrolysis voltage. Thus, the optimum concentration of sodium chloride is round about 100 ppm (corresponding to 61 ppm Cl^-). The decrease of electrolysis potential difference can be related to ohmic potential drop of the solution and/or to a decrease of the anode overpotential. It is to be noted that the cathode overpotential cannot take place in our case since no precipitate is formed on the cathode surface. The slight increase of electrolyte conductivity with

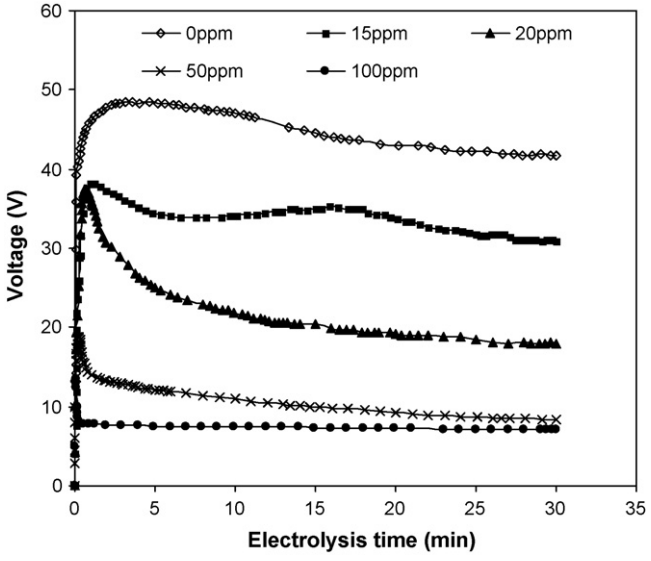

Fig. 1. Variation of electrolysis voltage with electrolysis time duration. Electrolyte: Na_2SO_4 (1 g/L) + x ppm NaCl, pH_i 5.4, $J = 0.5$ A/dm^2, $S_{TE} = 30$ cm^2, $d_{ie} = 4$ cm, aluminum electrodes.

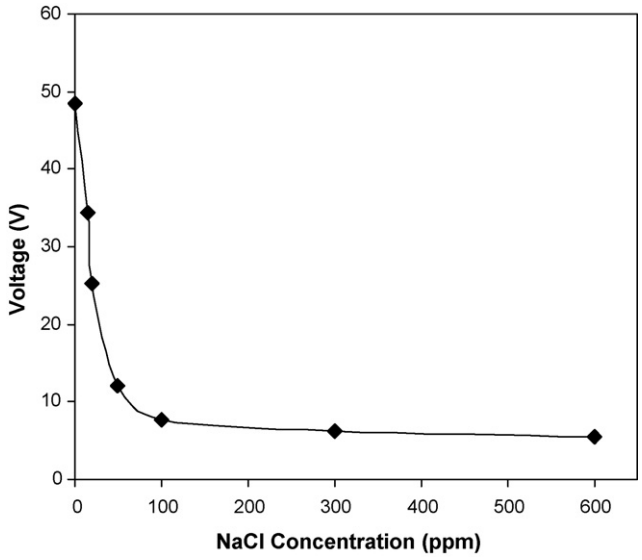

Fig. 2. Effect of NaCl dose on the electrolysis voltage. Electrolyte: Na_2SO_4 (1 g/L) + x ppm NaCl, t_e = 30 min, pH_i 5.4, J = 0.5 A/dm^2, S_{TE} = 30 cm^2, and d_{ie} = 4 cm, aluminum electrodes.

NaCl doses (measured conductivities of Na_2SO_4 based solutions linearly rise from 1.71 to 2.93 mS/cm when NaCl concentrations vary from 0 to 600 ppm) cannot explain the significant decrease of electrolysis voltage. Thus, this result has its roots in the anodic overpotential decrease. Moreover, the tiny variation of electrolysis voltage with NaCl doses exceeding 100 ppm maintains this hypothesis. Figs. 3 and 4 show, respectively, the evolution of anodic and cathodic potentials of aluminum electrodes during electrolysis tests. As can be seen, the anodic potential evolution plot (Fig. 3) is similar to that observed for electrolysis voltage (Fig. 1). Hence, it seems that the electrochemical behavior of the anode runs the whole studied system.

Fig. 5 shows optical micrographs of aluminum anodes after electrolyses in different NaCl-containing solutions. In NaCl-free solution, elongated craters with low distribution density (Fig. 5a)

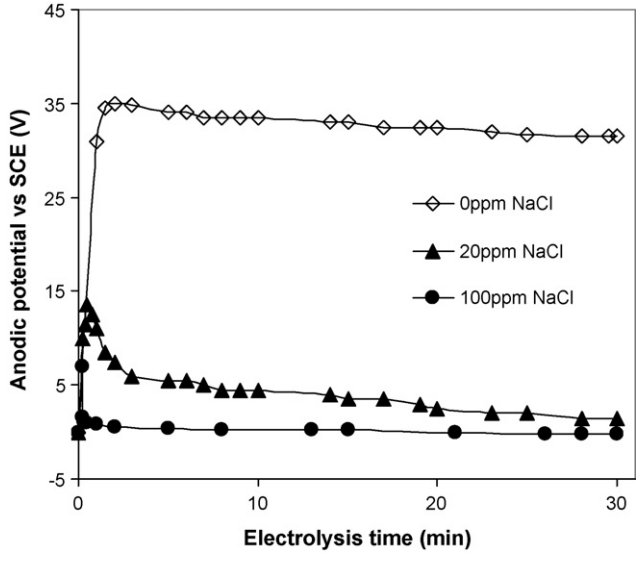

Fig. 3. Variation of anodic potential vs. SCE as a function of electrolysis time duration. Electrolyte: Na_2SO_4 (1 g/L) + x ppm NaCl, pH_i 5.4.

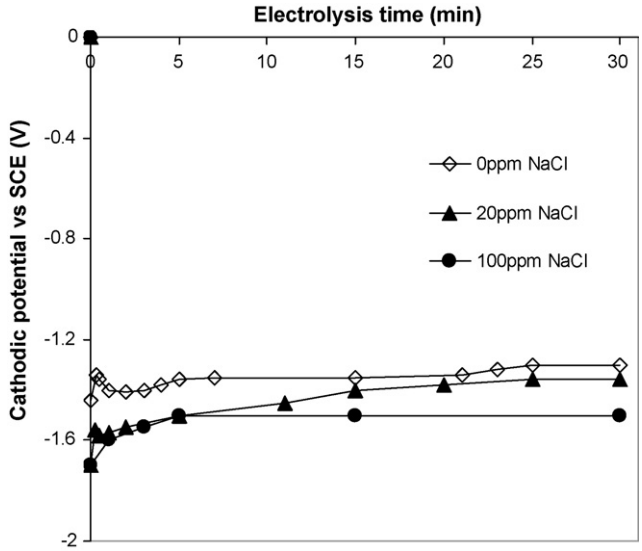

Fig. 4. Variation of cathodic potential vs. SCE as a function of electrolysis time. Electrolyte: Na_2SO_4 (1 g/L) + x ppm NaCl, pH_i 5.4.

appeared. In return, all the other anode surfaces exhibit pitting corrosion i.e. a localized form of attack upon the passive surface. Size and distribution of the rounded pits seem to be dependent on NaCl concentration. For NaCl doses increasing from 20 to 300 ppm, pits became finer and deeper, simultaneously their distribution density increased (Fig. 5b–e). At higher doses of NaCl, the opposite phenomenon is observed (Fig. 5f). Fig. 6 shows typical SEM micrography of a typical pit on anodic aluminum surface after electrolysis in 100 ppm NaCl solution.

Electrochemical behavior of aluminum was also studied, in Na_2SO_4 solutions containing 0 to 600 ppm NaCl, using the potentiodynamic polarization method. The current density response was converted to a logarithmic scale in order to show curve details in all the potential range considered. Fig. 7 illustrates some current density–potential curves obtained at a scan rate of 5 mV/s. Anodic polarization starting from the hydrogen evolution potential at −1800 mV/SCE and evolving towards 2500 mV/SCE was adopted. The observed corrosion potential of aluminum electrode in the NaCl-containing solutions is between about −1300 and −1100 mV versus SCE. Such results are in accordance with literature [29,30].

When comparing Fig. 7a to Fig. 7b and c, the absence of pitting corrosion in free-NaCl solution is noticed in the range of potential considered. The plateau of current density ($J \approx 0.03$ mA/cm^2) observed between E_{corr} and E_{pit} in Fig. 7b and c indicates aluminum dissolution through the oxide film (no pitting), whereas the sudden increase of the anodic current density indicates the change of aluminum dissolution mechanism to a pitting one [31,32]. In accordance with other works [22], the pitting potential E_{pit} (V) decreases with the logarithm of chloride concentration (ppm) as follow:

$$E_{pit} = 1.75 - 0.72 \log [Cl^-] \quad \text{with } R^2 = 0.99$$

Note that the above results are in agreement with those reported in several papers dealing with aluminum corrosion resistance in different media, especially halide ions-containing

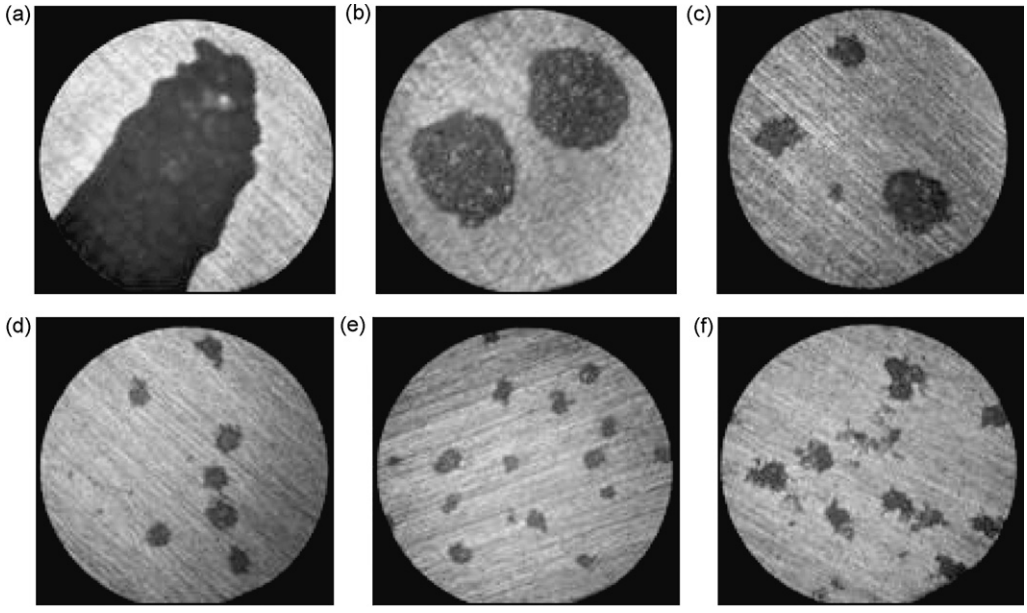

Fig. 5. Micrographs of aluminum anodes after electrolyses in different NaCl-containing solutions (magnification: 100×). Electrolyte: Na_2SO_4 (1 g/L) + (a) 0 ppm NaCl, (b) 20 ppm NaCl, (c) 50 ppm NaCl, (d) 100 ppm NaCl, (e) 300 ppm NaCl, (f) 600 ppm NaCl, pH_i 5.4, $J = 0.5$ A/dm^2, $S_{TE} = 30$ cm^2, $d_{ie} = 4$ cm, $t_e = 30$ min, aluminum electrodes.

solutions [29,33–40]. According to these works, aluminum surface is known to be covered by an oxide/hydroxide layer in neutral as well as in acidic and alkaline media although the oxide composition and structure are different. The breakdown of this spontaneous protective layer is believed to be responsible for the corrosion of aluminum or its electrodissolution when anodically polarized [29]. In accordance with amphoteric character of aluminum oxide, this film use to be rapidly dissolved in strong acidic or alkaline solutions. However, when solution pH is between *ca* 4 and 8.5, this layer is stable but undergoes localized attack (pitting dissolution) in halide anions presence, particularly chloride (Cl^-) [34]. When considering a Cl^- free solution (e.g. Na_2SO_4), the native oxide does not pit regardless of the potential applied [33]. In the other side, the presence of sulfate anions in Cl^- containing solution delays (i.e. raise the E_{pit} value) but not prevents the onset of pitting [35–38].

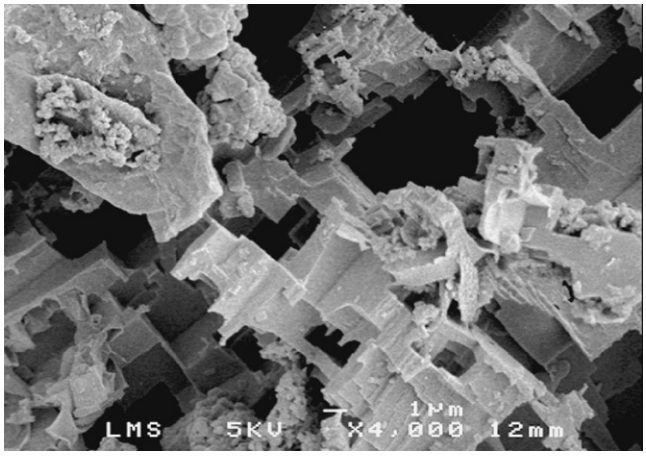

Fig. 6. SEM micrography of typical surface morphology of aluminum anode after electrolysis test in 100 ppm NaCl electrolyte.

4.2. Effect of pH

4.2.1. Effect of initial pH on the electrolysis voltage

The initial pH is one of the important factors affecting the performance of electrochemical process [41–45]. To examine its effect, a series of experiments were carried out using 100 ppm NaCl-containing solutions, with an initial pH varying in the range 2–12. Fig. 8 depicts the evolution of the electrolysis voltage as a function of the initial pH. A decrease of cell voltage is observed both at acidic ($2 < pH < 4$) and alkaline ($10 < pH < 12$) media whereas the pH effect is not significant in the range of 4–10. The electrolysis voltage decrease can be essentially correlated with the decrease of conductivity of the solutions (Fig. 8).

4.2.2. Evolution of the electrolyte pH during electrolysis

Fig. 9 illustrates the pH change of the bulk solution during electrolysis. As shown, as the initial pH of solution is slightly

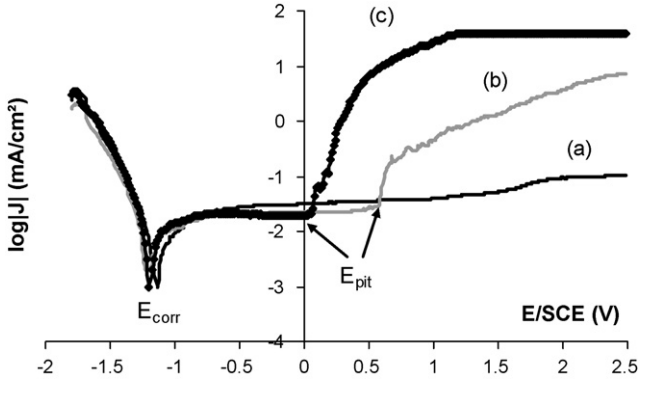

Fig. 7. Polarization curves at a scan rate of 5 mV/s in different NaCl-containing solutions. (a) 0 ppm, (b) 50 ppm and (c) 200 ppm. Scan rate: 5 mV/s, scan direction: from −1800 to 2500 mV/SCE.

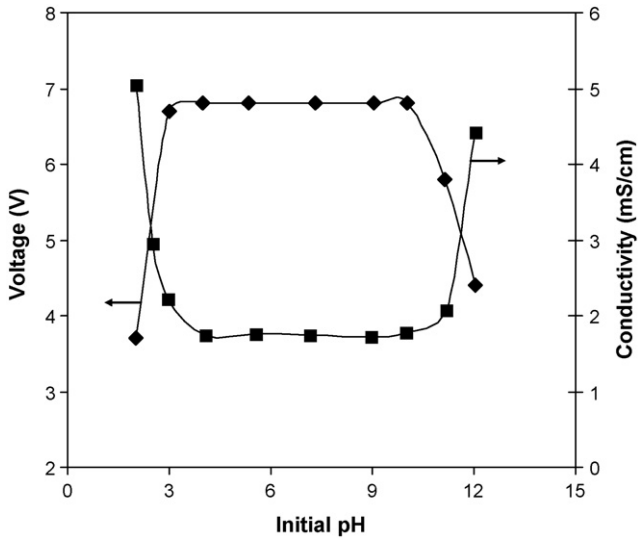

Fig. 8. Dependence of electrolysis voltage and initial conductivity vs. initial pH. Electrolyte: Na_2SO_4 (1 g/L) + 100 ppm NaCl, $J = 0.5$ A/dm^2, $S_{TE} = 30$ cm^2, $d_{ie} = 4$ cm, $t_e = 30$ min, aluminum electrodes.

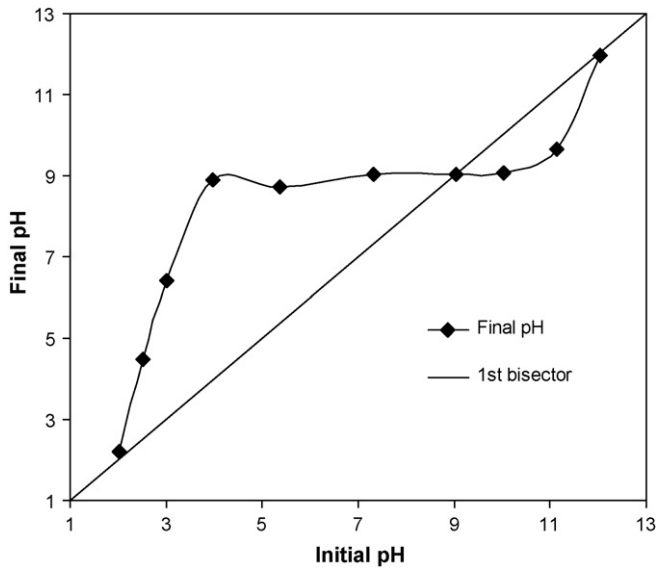

Fig. 10. Evolution of final pH vs. initial pH. Electrolyte: Na_2SO_4 (1 g/L) + 100 ppm NaCl, $J = 0.5$ A/dm^2, $S_{TE} = 30$ cm^2, $d_{ie} = 4$ cm, $t_e = 30$ min, aluminum electrodes.

acidic (pH_i 3 and 4.7), pH values rise during electrolysis process. However, in highly acidic electrolyte (pH_i 2), the alkalinity produced during electrolysis was not sufficient to increase the pH of the solution.

Fig. 10 depicts the electrolyte pH after electrolysis versus initial pH. As seen, when initial pH is acidic, final pH value rises and when initial pH is alkaline, final pH drops. Fig. 10 shows also that in highly acidic (pH 2) or alkaline solutions (pH 12), the pH remains unchanged. This invariability is attributed to the limited effects of phenomena allowing pH changes. For electrolyte at pH 9, the invariability of pH, observed elsewhere [14,18], is due to the fact that alkalizing phenomena offset the acidifying ones.

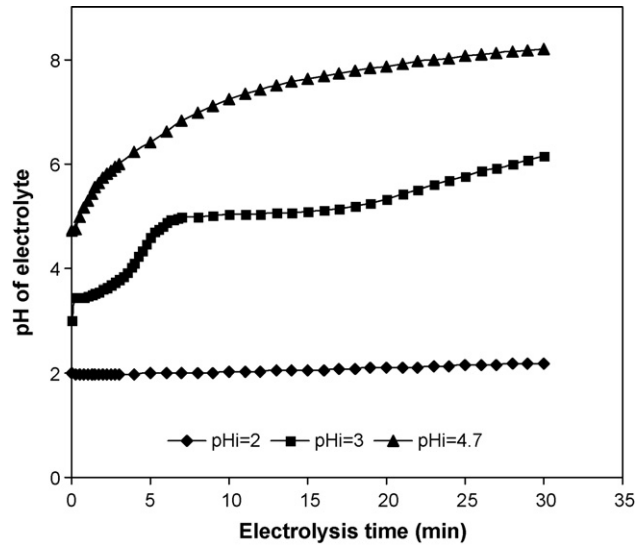

Fig. 9. Evolution of pH during electrolysis. Electrolyte: Na_2SO_4 (1 g/L) + 100 ppm NaCl, $J = 0.5$ A/dm^2, $S_{TE} = 30$ cm^2, $d_{ie} = 4$ cm, aluminum electrodes.

Regarding this pH variation during electrolysis with aluminum electrodes there is still a certain uncertainty as to its origin. In fact, several published accounts [6,18,23] attributed the pH increase to hydrogen evolution at the cathode (Eq. (2)). However, according to Chen et al. [14] this pH change can be from other mechanisms. One of them is the transfer of CO_2: CO_2 is over saturated in acidic aqueous electrolyte and can release from the medium owning to H_2 bubble disturbance, which causes a pH increase. In addition, these authors [14] reported that when some anions such as Cl^- and SO_4^{2-} are present in the electrolyte, they can exchange partly with OH^- in $Al(OH)_3$ to free OH^-, which also causes a pH increase.

Concerning the pH drop which occurs when the initial pH is above 9, it is attributed, as suggested by many investigators [14,23], to the dissolution reactions of aluminum and its hydroxide as $[Al(OH)_4]^-$ which are alkalinity consumers.

As far as we are concerned, further explanation will be given latter. Nevertheless, independently of the origins of the pH change during electrolysis with aluminum electrodes, some quite meaningful consequences connected with this pH evolution can be evoked here. First, since a pH increase occurs when the initial pH is acidic and a pH drop occurs when the initial pH is alkaline, EC using aluminum as electrode material acts as pH neutralization [14]. This finding is quite meaningful in EC application to wastewater treatment which can eliminate further pH adjustment of the effluent. Secondly, while effective chemical coagulation (using alum as a coagulant) is known to be achieved at pHs of 6–7 [46], EC can obviously work effectively over a much wider pH range [13,14]. Actually, this fact can be attributed to the ability of EC to neutralize wastewater pH. Thus, during EC, the pH value of the effluent will be brought closer to neutral, where effective coagulation has been reported. Finally, the pH increase of initially acidic effluents containing ionic metallic species (e.g. Cu^{2+}, Zn^{2+}, Ni^{2+}, Cr^{3+}, etc.) may induce their coprecipitation in the form of their corresponding

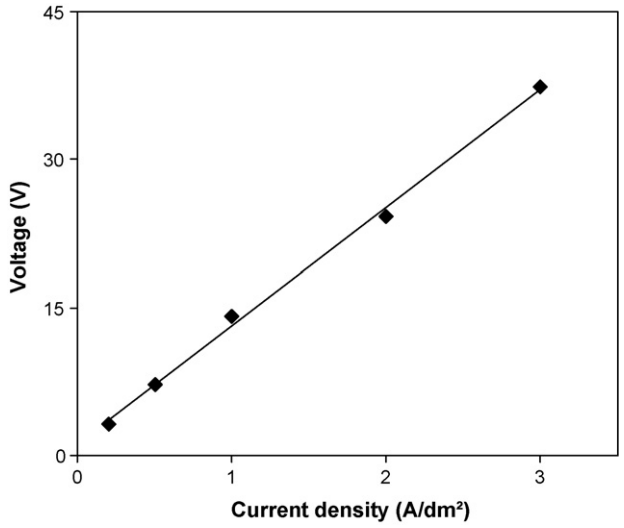

Fig. 11. Variation of electrolysis voltage as a function of current density. Electrolyte: Na_2SO_4 (1 g/L) + 100 ppm NaCl, pH_i 5.4, $S_{TE} = 30\,cm^2$, $d_{ie} = 4\,cm$, aluminum electrodes.

hydroxides. Obviously, electrolysis with aluminum electrodes offers to EC process significant potential for removing soluble heavy metals by electroprecipitation which acts synergistically with usual coagulation phenomena to remove pollutants from wastewaters.

4.3. Effect of current density on cell voltage

In all electrochemical processes, current density is the most important operating parameter. Fig. 11 depicts the evolution of electrolysis voltage with current density. As shown, the electrolysis voltage increases linearly with current density. Consequently, an increase of current density leads to an increase of power requirement. It is to be noted that the same linear evolution was observed by Chen et al. when considering restaurant wastewater [14].

The effect of electrode gap on the electrolysis voltage was investigated in 1 g/L Na_2SO_4 solution containing 100 ppm NaCl when d_{ie} ranging between 2 and 12 cm (not shown). For a current density of 0.5 A/dm^2, the electrolysis voltage U varies with electrode gap d_{ie} (cm) as follow:

$$U(\mathrm{V}) = 2.15\,d_{ie} - 1.15 \quad \text{with } R^2 = 0.98$$

The electrolysis voltage increases unsurprisingly with electrode gap owning to the ascent of the electrolyte resistance ($R = d_{ie}/\chi \cdot S_{TE}$). However, the significant increase recorded in this case is related to the low conductivity of the electrolyte (see Section 4.1).

4.4. Aluminum release during electrolysis: effect of operating parameters (NaCl, pH, J)

The study of aluminum release during electrolysis with aluminum electrodes is not only of scientific value but has also technological merits as the coagulant dosage is a key parameter for EC process. Indeed, since coagulation is achieved by charge neutralization and destabilization of negatively charged colloids by cationic hydrolysis products of Al^{3+} ions, excess dosage of coagulant can give charge reversal and restabilisation of colloids. Although several studies claimed that aluminum dosage strongly affect process efficiency, no clues as to the effect of different operating parameters on the extent of coagulant release were found. Thus, the effects of NaCl concentration, electrolyte pH and current density are now systematically investigated.

In the following paragraphs, the amount of released aluminum includes both the dissolved aluminum and that precipitated as $Al(OH)_3$.

Fig. 12 shows the amount of released aluminum in the aqueous solution as a function of NaCl concentration of the electrolyte. One can observe that the amount of aluminum generated increases rapidly as the NaCl dose varies from 0 to 15 ppm. Subsequently, the quantity of Al^{3+} (coagulant) produced becomes almost constant. Moreover, the amount of aluminum generated during electrolysis exceeds the theoretical value calculated from Faraday's law. The current efficiency of aluminum dissolution is in our case about 175%. Many works have displayed prominently such excess but there was a wide spread in its measured value. Indeed, the current efficiency values reported in the literature ranged between 109 and 215% [14,47–50]. At least part of the disagreements in the published data may be the result of different conditions under which the experiments were carried out (electrolyte pH and composition, electrolysis duration, etc.). Concerning, the origin of such an excess many explanations have been given in the published accounts. According to several authors [14,23,43,49,51] chemical attack of both anode and cathode can occur due to the acidity and alkalinity produced at their vicinity, respectively:

- at the anode vicinity:

$$2Al + 6H^+ \rightarrow 2Al^{3+} + 3H_2 \quad (7)$$

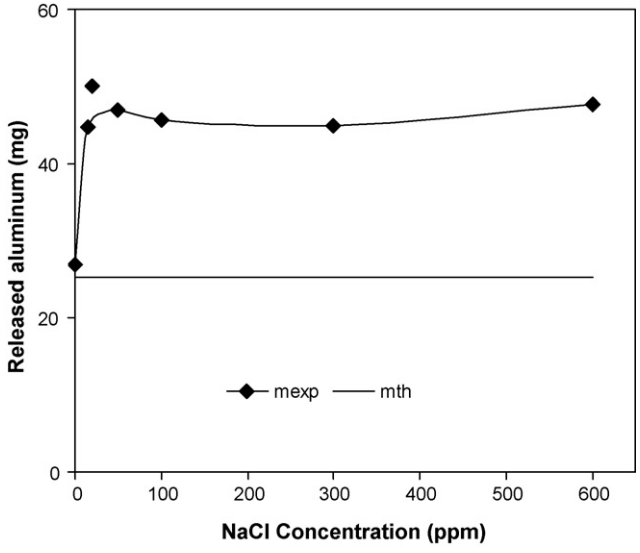

Fig. 12. Variation of the amount of aluminum released as a function of NaCl concentration. Electrolyte: Na_2SO_4 (1 g/L) + x ppm NaCl, pH_i 5.4, $J = 0.5$ A/dm^2, $S_{TE} = 30\,cm^2$, $d_{ie} = 4\,cm$, $t_e = 30$ min, aluminum electrodes.

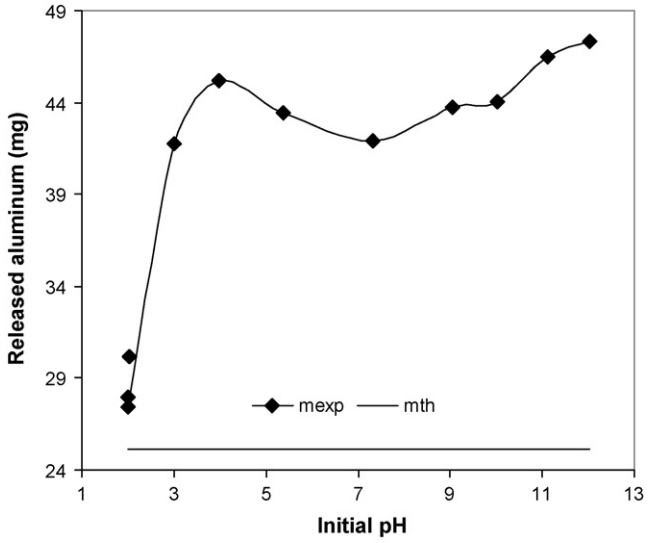

Fig. 13. Variation of the amount of aluminum released as a function of initial pH. Electrolyte: Na_2SO_4 (1 g/L) + 100 ppm NaCl, $J = 0.5$ A/dm^2, $S_{TE} = 30$ cm^2, $d_{ie} = 4$ cm, $t_e = 30$ min, aluminum electrodes.

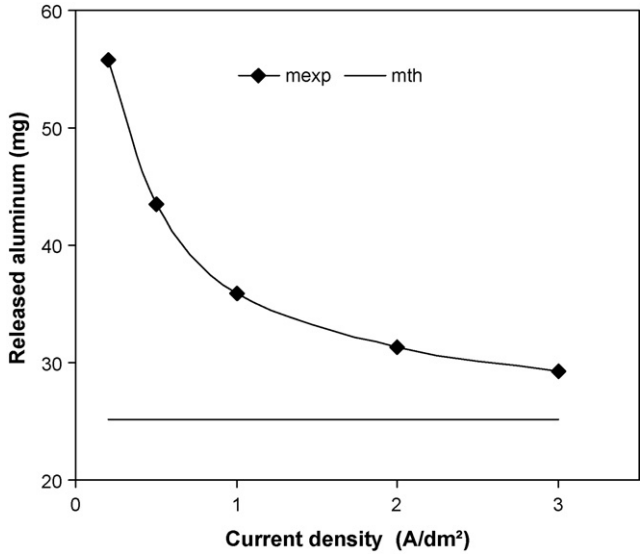

Fig. 14. Variation of the amount of aluminum generated as a function of current density at constant charge loading ($Q = 270$ C). Electrolyte: Na_2SO_4 (1 g/L) + 100 ppm NaCl, pH_i 5.4, $S_{TE} = 30$ cm^2, $d_{ie} = 4$ cm, $t_e = 30$ min, aluminum electrodes.

- at the cathode vicinity:

$$2Al + 6H_2O + 2OH^- \rightarrow 2[Al(OH)_4]^- + 3H_2 \quad (8)$$

$$Al(OH)_3 + OH^- \rightarrow [Al(OH)_4]^- \quad (9)$$

This view point was not shared by others who suggested that efficiencies exceeding 100% could be explained by "pitting corrosion" of anode caused by chloride ions present in the medium [47,48,52]. Our results concerning this topic will be given subsequently.

Fig. 13 shows the amount of released aluminum versus the initial electrolyte pH. A sharp increase of the released amount is clearly shown in the pH range 2–3. Beyond pH 3, the variation of the amount of dissolved aluminum seems to be not very significant. The amount of aluminum generated during electrolysis always exceeds that theoretical calculated from Faraday's law.

Fig. 14 displays the effect of current density on the amount of released aluminum at a constant charge loading Q equal to 270 C. This charge corresponds to 5.6 Faraday/m^3 of electrolyte according to our experimental design. As recorded previously, the quantity of released aluminum always exceeds that determined by the Faraday's law. Furthermore, it is worthwhile to note that the difference between the experimental and theoretical amounts of released aluminum is more important as the current density is lower (Fig. 14).

In order to examine these findings, complementary electrolyses have been envisaged to discriminate the contribution of the cathodic and anodic processes as well as the chemical phenomena on the amount of released aluminum. Therefore, electrolyses with different cell configurations were carried out.

4.4.1. Configuration 1: uncompartmentalized cell with an aluminum anode and a platinized titanium cathode

The variation of the amount of anodically generated aluminum versus current density (Fig. 15) depicts no noticeable difference between theoretical and experimental quantities of coagulant (Al^{3+}) released. Thus, aluminum dissolves especially according to reaction (1). Consequently, neither chemical dissolution of aluminum by the acidity produced at the interface anode/electrolyte (see Eq. (7)) [14,23,43,49,51] nor the pitting corrosion of anode by Cl^- ions [47,48,52] are significant to explain the excess of released aluminum observed previously.

4.4.2. Configuration 2: uncompartmentalized cell with a platinized titanium anode and an aluminum cathode

Fig. 16 provides good evidence that aluminum dissolves at the cathode. According to the Pourbaix diagram [53], aluminum

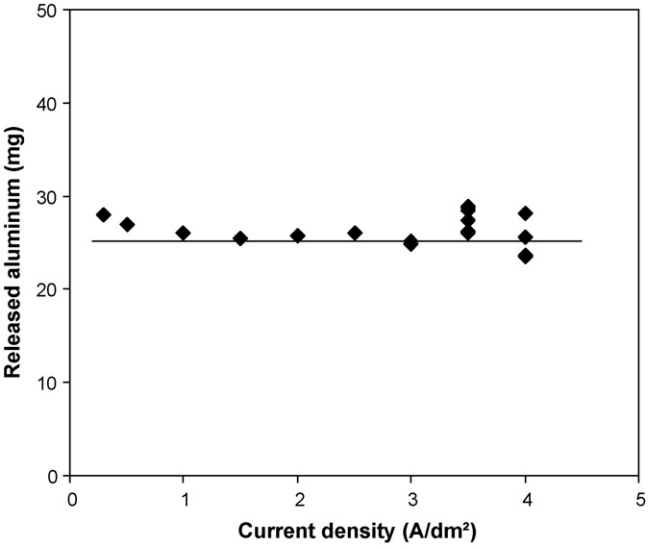

Fig. 15. Variation of the amount of anodically generated aluminum as a function of current density at constant charge loading ($Q = 270$ C). Electrolyte: Na_2SO_4 (1 g/L) + 100 ppm NaCl, pH_i 5.4, $S_{TE} = 30$ cm^2, $d_{ie} = 4$ cm, anode: aluminum, cathode: platinized titanium.

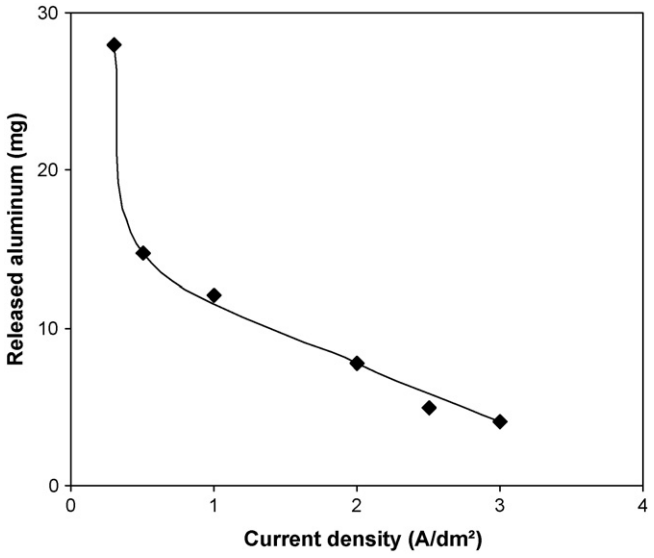

Fig. 16. Variation of the amount of released aluminum at the cathode as a function of current density at constant charge loading ($Q = 270$ C). Electrolyte: Na_2SO_4 (1 g/L) + 100 ppm NaCl, pH_i 5.4, $S_{TE} = 30\ cm^2$, $d_{ie} = 4$ cm, anode: platinized titanium, cathode: aluminum.

is passive in the pH range of 4–8.5. Beyond this range, aluminum corrosion occurs in aqueous solutions since its oxide is soluble either in acidic and alkaline media, yielding to Al^{3+} ions in the former and $[Al(OH)_4]^-$ ions in the latter. During electrolysis, the significant increase of the local pH at the cathode vicinity due to hydrogen evolution (Eq. (2)) induces "chemical" attack of aluminum and its hydroxide film, according to Eqs. (8) and (9). Unlike the anodic dissolution process, the cathode undergoes a generalized dissolution as shown by SEM image taken after electrolysis (Fig. 17). This implies that as OH^- ion concentration rises at the cathode vicinity, uniform thinning of the aluminum electrode overwhelms the pitting corrosion by Cl^- ions attack. This observation is in agreement with findings of some investigations dealing with corrosion of aluminum in alkaline media [40,54].

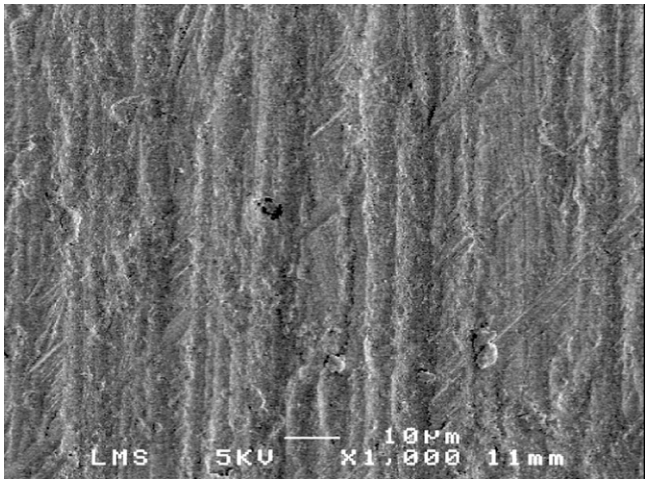

Fig. 17. SEM micrography of typical surface morphology of aluminum cathode after electrolysis test.

Furthermore, as the current density decreases the amount of aluminum generated increases (Fig. 16). Since electrolyses were carried out at constant charge loading, the duration time of electrolysis is as long as current density is low. Consequently, the contact time of the cathode with the local alkalinity produced at its surface during H_2 evolution is longer. This gives rise to the chemically generated aluminum.

It is interesting to point out that the shape of the curve, showing the amount of dissolved aluminum at the cathode (Fig. 16), is similar to that previously observed for the global quantity of released aluminum (see Fig. 14). Keeping in mind that the quantity of aluminum produced by electro-oxidation of the anode is practically equal to that theoretical and almost insensitive to current density (see Fig. 15), the increase of the total quantity of aluminum released during electrolysis (see Fig. 14) could be ascribed to that "chemically" dissolved at the cathode (see Fig. 16).

4.4.3. Configuration 3: electrolyses in compartmentalized cell with two aluminum electrodes

For this configuration, anolyte and catholyte were separated by a cation exchange membrane. The results obtained (Fig. 18) reveal that the anodic process is slightly "acidifying". This acidity is mainly due to the hydrolysis of the Al^{3+} ions produced at the anode (see Eqs. (4)–(6))

Electro-oxidation of water (Eq. (3)) as acidifying anodic reaction mentioned by earlier papers [13,14,18,21,23] cannot be retained in regard to our results. In fact, since the aluminum anodic dissolution efficiency is close to unity and does not depend on the applied current density, this secondary reaction cannot take place or is at least negligible.

Fig. 18 shows also that cathodic process is alkalizing. This alkalinity resulted from hydrogen evolution reaction (see Eq. (2)).

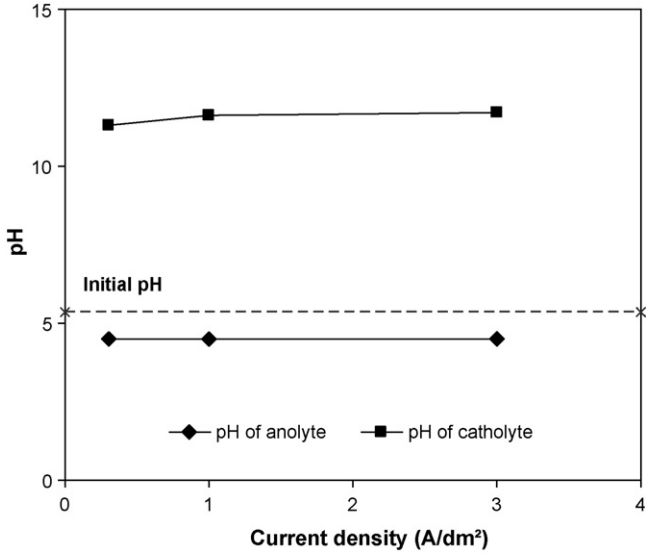

Fig. 18. Final pH of the anolyte and catholyte as a function of current density at constant charge loading ($Q = 270$ C). Electrolyte: Na_2SO_4 (1 g/L) + 100 ppm NaCl, pH_i 5.4, $S_{TE} = 30\ cm^2$, $d_{ie} = 4$ cm, aluminum electrodes.

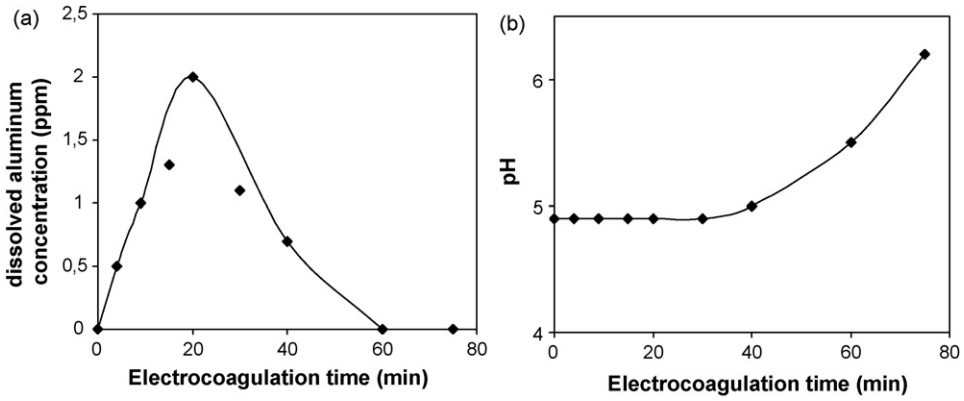

Fig. 19. Dissolved aluminum concentration (a) and pH (b) evolutions of the synthetic wastewater with electrocoagulation time. $J = 0.5$ A/dm^2, $S_{TE} = 54$ cm^2, $d_{ie} = 4$ cm, aluminum electrodes.

At this stage, it can be concluded that during electrolysis, the global amount of coagulant (Al^{3+}) generated in the electrolyte has two main origins: (i) electrochemical oxidation of the anode and (ii) "chemical" attack of the cathode due to local alkalinity of the electrolyte.

4.5. Electrocoagulation tests

Taking into account the pH increase during electrolyses with aluminum electrodes, potentiality of EC process for removing soluble heavy metallic species is now tested considering a synthetic wastewater containing Ni^{2+}, Cu^{2+} and Zn^{2+} ions (see composition Section 2). Particular focus was given to removal efficiency of metallic species.

Fig. 19 shows the dissolved aluminum concentration (a) and the electrolyte pH (b) evolutions during electrocoagulation. The amount of aluminum rises in the beginning of the treatment and reaches a maximum of 2 ppm at 20 min of electrolysis and then decreases (Fig. 19a). So, residual aluminum remains at low level owing to the precipitation of $Al(OH)_3$ during electrocoagulation treatment. Consequently, residual Al^{3+} species do not contaminate the electrolyte. The pH of the medium remains quasi-constant at the beginning of electrocoagulation and then increases (Fig. 19b). The invariability of pH – in contrast with its increase observed in Fig. 9 – is due to the precipitation of metallic species which consume the alkalinity produced at the cathode.

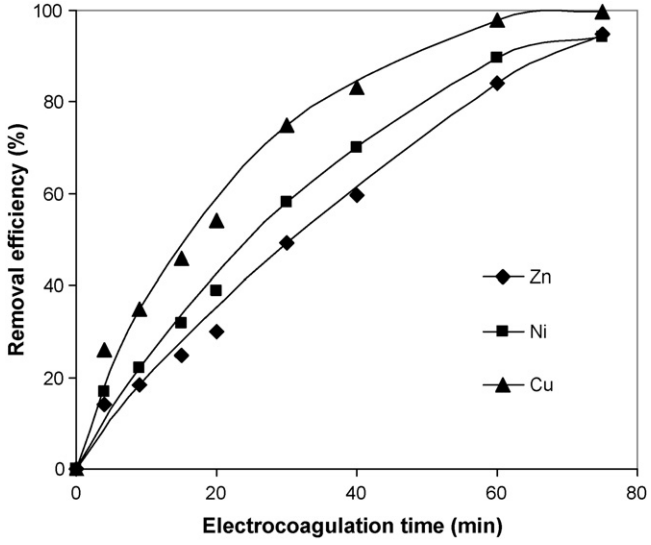

Fig. 20. Effect of electrocoagulation time on the removal efficiencies of Ni(II), Cu(II) and Zn(II). $J = 0.5$ A/dm^2, $S_{TE} = 54$ cm^2, $d_{ie} = 4$ cm, aluminum electrodes.

The time dependence of removal efficiency by EC process is depicted in Fig. 20. The removal efficiency (%) was calculated

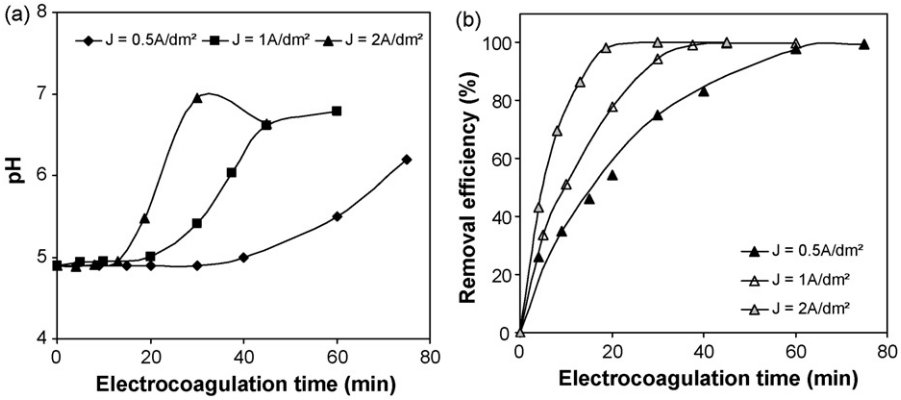

Fig. 21. "Wastewater" pH (a) and removal efficiency of Cu(II) (b) evolutions with electrocoagulation time at different current densities. $S_{TE} = 54$ cm^2, $d_{ie} = 4$ cm, aluminum electrodes.

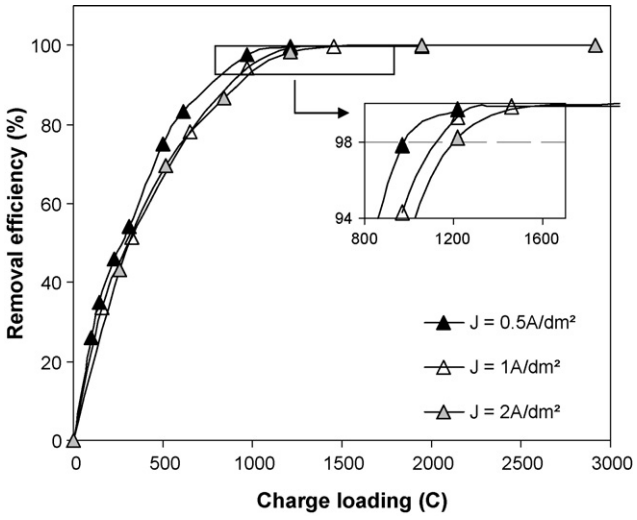

Fig. 22. Variation of copper removal efficiency as a function of charge loading for different current densities, $S_{TE} = 54\ cm^2$, $d_{ie} = 4$ cm, aluminum electrodes.

as follows:

$$RE = \left(\frac{C_0 - C_f}{C_0}\right) \times 100$$

The removal efficiencies of the different metallic ions (Ni^{2+}, Cu^{2+} and Zn^{2+}) increase with electrocoagulation time. Moreover, ionic species precipitate in the following order: Cu, Ni, Zn according to their solubility constant value [55]. It can be seen that a removal efficiency (i) up to 40 and 60%, for Zn and Cu species respectively, is obtained within 20 min of the process and (ii) around 100% is reached at approximately 75 min of EC treatment.

The effect of current density on "wastewater" pH evolution and removal efficiencies were also studied. Electrocoagulation tests were carried out at 0.5, 1 and 2 A/dm^2. As shown in Fig. 21a, the pH invariability duration during electrolysis decreases as current density increases. In addition, the required EC time falls, for all metallic ions, as the current density increases. Fig. 21b illustrates this fact in the case of Cu^{2+} ions. The same trend was observed for Ni^{2+} and Zn^{2+} species (not shown). In the case of copper (Fig. 21b), the electrocoagulation time needed to achieve a residual concentration of 1 mg/L – equivalent to 98% of removal efficiency – is around 60, 34 and 18 min under 0.5, 1 and 2 A/dm^2, respectively. Consequently, an increase of the current density notably reduces the EC required time without inducing a strong increase of the charge loading, however. Indeed, a small charge loading difference is observed to access to the same removal efficiency (98%) (Fig. 22). This charge loading difference could not be attributed to electrochemical parasite reactions as reported by others [21,56] but might be relied to precipitation kinetics of metallic hydroxides. This is in agreement with the results in Section 4.4 which shown the absence of electrochemical parasite reactions in particular water oxidation. At this stage, it is noteworthy that current density is not an appropriate parameter for assessing metallic ions removal from wastewater and thereby charge loading should be considered as a design parameter of the process. The above conclusion shows the advantage of using relatively high current density in order to reduce the EC processing time and thus the EC equipment.

5. Conclusion

In this study, the behavior of aluminum as electrode material in EC process has been investigated. The effect of different operating parameters (electrolyte composition, pH, current density, etc.) on aluminum release and cell voltage during electrolysis have been studied. The wide range of experiments performed provided evidence that:

- the electrolyte should contain a minimum Cl^- concentration of about 60 ppm to breakdown the anodic passive film and remarkably reduce the cell voltage during EC;
- the electrolysis with aluminum electrodes acted as pH neutralization;
- no secondary electrochemical reaction, specially oxygen evolution, took place at the aluminum anode and then the anodic dissolution efficiency was unit;
- the cathodic electrochemical process (hydrogen evolution) induced a chemical attack of aluminum cathode which contributed significantly to the global amount of aluminum released.

By using different reactor configurations, we were able to discriminate the amount of aluminum produced at each electrode.

An electrocoagulation treatment of a synthetic wastewater was successfully implemented from removal efficiency point of view. An increase of the current density notably reduced the electrocoagulation required time for the treatment without inducing a strong increase of the charge loading.

In a subsequent work, more details on electrocoagulation process as sedimentation kinetics of metallic sludge – in relation with the amount of aluminum released – will be reported.

Acknowledgments

The authors wish to acknowledge financial support by the Tunis International Center for Environmental Technologies (CITET). Authors also would like to thank Pr. Sami SAYEDI, the scientific coordinator of this project: "PRF Eau 2: Petites stations de traitement: Approches innovatrices "alternatives" ".

Thanks are due to Dr. A. Vidonne (University of Franche-Comté – France) for his assistance.

References

[1] K. Rajeshwar, J. Ibanez, G.M. Swain, Electrochemistry and the environment, J. Appl. Electrochem. 24 (1994) 1077–1091.
[2] L. Antropov, Theoretical Electrochemistry, Mir, Moscow, 1977.
[3] C.Y. Hu, S.L. Lo, W.H. Kuan, Effects of co-existing anions on fluoride removal in electrocoagulation (EC) process using aluminum electrodes, Water Res. 37 (2003) 4513–4523.
[4] N.S. Abuzaid, A. Bukhari, Z.M. Al-Hamouz, Ground water coagulation using soluble stainless steel electrodes, Adv. Environ. Res. 6 (2002) 325–333.

[5] H. Bergmann, A. Rittel, T. Iourtchouk, K. Schoeps, K. Bouzek, Electrochemical treatment of cooling lubricants, Chem. Eng. Process. 42 (2003) 105–119.
[6] E.A. Vik, D.A. Carlos, A.S. Eikum, E.T. Gjessing, Electrocoagulation of potable water, Water Res. 18 (1984) 1355–1360.
[7] Ü.B. Öğütveren, S. Koparal, Electrocoagulation for oil–water emulsion treatment, J. Environ. Sci. Health A 32 (1997) 2507–2520.
[8] J.S. Do, M.L. Chen, Decolorization of dye-containing solutions by electrocoagulation, J. Appl. Electrochem. 24 (1994) 785–790.
[9] A. Gürses, M. Yalçın, C. Doğar, Electrocoagulation of some reactive dyes: a statistical investigation of some electrochemical variables, Waste Manage. 22 (2002) 491–499.
[10] Ü.B. Öğütveren, N. Gonen, A.S. Koparal, Removal of dye stuffs from waste water: electrocoagulation of Acilan Blau using soluble anode, J. Environ. Sci. Health A 27 (1992) 1237–1247.
[11] S.H. Lin, C.F. Peng, Treatment of textile wastewater by electrochemical method, Water Res. 28 (1994) 277–282.
[12] M.F. Pouet, A. Grasmick, Urban wastewater treatment by electrocoagulation and flotation, Water Sci. Technol. 31 (1995) 275–283.
[13] G. Chen, X. Chen, P.L. Yue, Electrocoagulation and electroflotation of restaurant wastewater, J. Environ. Eng. 126 (2000) 858–863.
[14] X. Chen, G. Chen, P.L. Yue, Separation of pollutants from restaurant wastewater by electrocoagulation, Sep. Purif. Technol. 19 (2000) 65–76.
[15] J.R. Parga, D.L. Cocke, J.L. Valenzuela, J.A. Gomes, M. Kesmez, G. Irwin, H. Moreno, M. Weir, Arsenic removal via electrocoagulation from heavy metal contaminated groundwater in La Comarca Lagunera México, J. Hazard. Mater. B 124 (2005) 247–254.
[16] J. Mrozowski, J. Zielinski, Studies of zinc and lead removal from industrial wastes by electrocoagulation, Environ. Prot. Eng. 9 (1983) 77–85.
[17] P.R. Kumar, S. Chaudhari, K.C. Khilar, S.P. Mahajan, Removal of arsenic from water by electrocoagulation, Chemosphere 55 (9) (2004) 1245–1252.
[18] N. Adhoum, L. Monser, N. Bellakhal, J.E. Belgaied, Treatment of electroplating wastewater containing Cu^{2+}, Zn^{2+} and Cr(VI) by electrocoagulation, J. Hazard. Mater. B 112 (2004) 207–213.
[19] M.Y.A. Mollah, R. Schennach, J.R. Parga, D.L. Cocke, Electrocoagulation (EC)-science and applications, J. Hazard. Mater. B 84 (2001) 29–41.
[20] P.K. Holt, G.W. Barton, C.A. Mitchell, The future for electrocoagulation as a localised water treatment technology, Chemosphere 59 (2005) 355–367.
[21] M.Y.A. Mollah, P. Morkovsky, J.A.G. Gomes, M. Kesmez, J. Parga, D.L. Cocke, Fundamentals, present and future perspectives of electrocoagulation, J. Hazard. Mater. B 114 (2004) 199–210.
[22] Z. Szklarska-Smialowska, Pitting Corrosion of Metals, NACE, Houston, 1986.
[23] M. Kobya, H. Hiz, E. Senturk, C. Aydiner, E. Demirbas, Treatment of potato chips manufacturing wastewater by electrocoagulation, Desalination 190 (2006) 201–211.
[24] L.D. Benefield, J.F. Judkins, B.L. Weand, Process Chemistry for Water and Wastewater Treatment, Prentice-Hall Inc., New Jersey, 1982.
[25] M. Bayramoglu, M. Kobya, O.T. Can, M. Sozbir, Operating cost analysis of electrocoagulation of textile dye wastewater, Sep. Purif. Technol. 37 (2004) 117–125.
[26] D.T. Richens, The Chemistry of Aqua Ions, Wiley, Chichester, 1997.
[27] J. Duan, J. Gregory, Coagulation by hydrolysing metal salts, Adv. Colloid Interface Sci. 100–102 (2003) 475–502.
[28] H. De Hek, R.J. Stol, P.L. De Bruyn, Hydrolysis-precipitation studies of aluminum (III) solutions. 3. The role of the sulfate ion, J. Colloid Interface Sci. 64 (1978) 72–89.
[29] T. Kıyak, M. KabasakaloKlu, Anodic behavior of cathodically pretreated aluminum electrode, Appl. Surf. Sci. 140 (1999) 33–45.
[30] J. Radošević, M. Kliškić, P. Dabić, R. Stevanović, A. Despić, Processes on aluminium on the negative side of the open-circuit potential, J. Electroanal. Chem. 277 (1990) 105–119.
[31] D.M. Dražić, J.P. Popić, Corrosion rates and negative difference effects for Al and some alloys, J. Appl. Electrochem. 29 (1999) 43–50.
[32] L. Tomcsányi, K. Varga, I. Bartik, H. Horányi, E. Maleczki, Electrochemical study of the pitting corrosion of aluminium and its alloys. II. Study of the interaction of chloride ions with a passive film on aluminium and initiation of pitting corrosion, Electrochim. Acta 34 (1989) 855–859.
[33] C.M. Johnson, F.D. Wall, J.C. Barbour, M.A. Martinez, A study of localized corrosion in Al resulting from the controlled introduction of Cl, Mater. Res. Soc. Symp. Proc. 781E (2003) Z2.9.1–Z2.9.6.
[34] J.W.J. Silva, A.G. Bustamante, E.N. Codaro, R.Z. Nakazato, L.R.O. Hein, Morphological analysis of pits formed on Al 2024-T3 in chloride aqueous solution, Appl. Surf. Sci. 236 (2004) 356–365.
[35] K.H. Na, Su-Il Pyun, Effect of sulphate and molybdate ions on pitting corrosion of aluminium by using electrochemical noise analysis, J. Electroanal. Chem. 596 (2006) 7–12.
[36] W.J. Lee, S.I. Pyun, Effects of sulphate ion additives on the pitting corrosion of pure aluminium in 0.01 M NaCl solution, Electrochim. Acta 45 (2000) 1901–1910.
[37] Z. Szklarska-Smialowska, Pitting corrosion of aluminium, Corros. Sci. 41 (1999) 1743–1767.
[38] W.J. Rudd, J.C. Scully, The function of the repassivation process in the inhibition of pitting corrosion on aluminium, Corros. Sci. 20 (1980) 611–631.
[39] J. Bernard, M. Chatenet, F. Dalard, Understanding aluminum behaviour in aqueous alkaline solution using coupled techniques. Part I. Rotating ring-disk study, Electrochim. Acta 52 (2006) 86–93.
[40] A. Kolics, J.C. Polkinghorne, A. Wieckowski, Adsorption of sulfate and chloride ions on aluminum, Electrochim. Acta 43 (1998) 2605–2618.
[41] S.H. Lin, M.L. Chen, Treatment of textile wastewater by electrochemical methods for reuse, Water Res. 31 (1997) 868–876.
[42] M. Kobya, O.T. Can, M. Bayramoglu, Treatment of textile wastewaters by electrocoagulation using iron and aluminum electrodes, J. Hazard. Mater. B100 (2003) 163–178.
[43] O.T. Can, M. Bayramoglu, M. Kobya, Decolorization of reactive dye solutions by electrocoagulation using aluminum electrodes, Ind. Eng. Chem. Res. 42 (2003) 3391–3396.
[44] N. Daneshvar, H. AshassSorkhabi, A. Tizpar, Decolorization of orange II by electrocoagulation method, Sep. Purif. Technol. 31 (2003) 153–162.
[45] D. Elemér, Experiments aimed at the removal of phosphate by electrochemical methods, Water Res. 12 (1978) 1113–1116.
[46] R.L. Sanks, Water Treatment Plant Design, Butterworth–Heinemann, Stoneham, MA, 1978.
[47] F. Shen, P. Gao, X. Chen, G. Chen, Electrochemical removal of fluoride ions from industrial wastewater, Chem. Eng. Sci. 58 (2003) 987–993.
[48] N. Mameri, A.R. Yeddou, H. Lounici, D. Belhocine, H. Grib, B. Bariou, Defluoridation of septentrional Sahara water of North Africa by electrocoagulation process using bipolar aluminium electrodes, Water Res. 32 (1998) 1604–1612.
[49] J.C. Donini, J. Kan, J. Szynkarczuk, T.A. Hassan, K.L. Kar, The operating cost of electrocoagulation, Can. J. Chem. Eng. 72 (1994) 1007–1012.
[50] L. Sánchez Calvo, J.P. leclerc, G. Tanguy, M.C. Cames, G. Paternotte, G. Valentin, A. Rostan, F. Lapicque, An electrocoaguhtion unit for the purification of soluble oil wastes of high COD, Environ. Prog. 22 (2003) 57–65.
[51] O.T. Can, M. Kobya, E. Demirbas, M. Bayramoglu, Treatment of the textile wastewater by combined electrocoagulation, Chemosphere 62 (2006) 181–187.
[52] M. Khemis, J.P. Leclerc, G. Tanguy, G. Valentin, F. Lapicque, Treatment of industrial liquid wastes by electrocoagulation: experimental investigations and an overall interpretation model, Chem. Eng. Sci. 61 (2006) 3602–3609.
[53] M. Pourbaix, Atlas of Electrochemical Equilibria in Aqueous Solution, 2nd ed., Pergamon Press, Houston, 1974.
[54] W.J. Lee, S.I. Pyun, Effects of hydroxide ion addition on anodic dissolution of pure aluminium in chloride ion-containing solution, Electrochim. Acta 44 (1999) 4041–4049.
[55] R.C. Weast, CRC Handbook of Chemistry and Physics, 58th ed., CRC Press, USA, 1977–1978.
[56] J.P.F. Koren, U. Syversen, State of the art electroflocculation, Filtr. Sep. 32 (1995) 146–156.